Comparative Study of Annealed and High Temperature Grown ITO and AZO Films for Solar Energy Applications

Diego Alonso-Álvarez[1], Lourdes Ferre Llin[2], Alexander Mellor[1], Douglas J. Paul[2] and Nicholas J. Ekins-Daukes[1]

[1]Imperial College London, Department of Physics, London SW7 2AZ, United Kingdom

[2]University of Glasgow, School of Engineering, Glasgow G12 8LT, United Kingdom

ABSTRACT

We present the optical and electrical properties of ITO and AZO films fabricated directly on silicon substrates under several growth and annealing temperatures, as well as their potential performance when used as low emissivity coatings in hybrid photovoltaic-thermal systems. We use broadband spectroscopic ellipsometry measurements (from 300 nm to 20 μm) to obtain a consistent model for the permittivity of each of the films. The best performance is found using the properties of the ITO film grown at 250 ºC, with a state of the art resistivity of 0.2 mΩ-cm and an optimized thickness of 75 nm which leads to an estimated 50% increase in the extracted power compared to a standard diffused silicon solar cell. The Hall mobility and resistivity measurements of all the films are also provided, complementing and supporting the observed optical properties.

INTRODUCTION

Transparent conductive oxides (TCO) are an integral part of modern electronic devices [1]. They are an essential component of displays and touchscreens in tablets and mobile phones. They are also key in light emitting diodes as well as in photovoltaics (PV), forming the front electrode in many solar cell technologies, such as in thin film devices (CdTe, CIGS and organic) or crystalline silicon heterojunction (SHJ) solar cells [2]-[4]. For solar energy, harvesting TCOs must have (a) very high transparency over the solar spectral range, and at the same time they must possess (b) excellent electrical transport properties. A more recent application is their use as low emissivity coatings for hybrid PV-thermal (PV-T) solar systems to keep the heat inside the solar cell and rise its temperature. In this case a third property, (c) low emissivity in the thermal range (5-20 μm), is also required. On the other hand, the electrical power produced by photovoltaic devices is fundamentally lower at the usual working temperatures of hybrid PV-T systems (60-100 ºC), dropping at around 0.42 %/ºC in typical silicon solar cells with respect the specifications at 25 ºC. However, the choice of a photovoltaic technology with low thermal coefficients (such as SHJ or CdTe) and the use of solar cells designed to work at high temperature should minimize the detrimental effect. Nowadays, PV-T systems which operate at higher working temperatures are based on evacuated tubes, where the solar cells are directly attached to the heat exchanger without any type of encapsulation. In those systems, convective losses are mostly suppressed and radiative losses can be reduced by tuning the properties (thicknesses of the layers, composition and dopant densities) of the coatings deposited directly into the solar cells.

In this work, we study the two most common TCOs, indium tin oxide (ITO) and aluminum zinc oxide (AZO) with this latter application in mind. Two sets of films deposited on silicon were studied for each of the materials: first set grown at different temperatures from room temperature to 350ºC, and second set grown at room temperature and then annealed up to 800^{o}C.

EXPERIMENT

Experimental details

The films were 100 nm thick and grown on an Angstrom RF magnetron sputtering system. Details of the growth conditions and structural characterization can be found elsewhere [5]. Samples of the two

materials were grown at room temperature (RT), 150 ºC, 250 ºC and 350 ºC. Five annealing temperatures were used for the samples that were grown at RT: 400 ºC, 500 ºC, 600 ºC, 700 ºC and 800 ºC, and the annealing time was 3 min in all cases under N_2 atmosphere.

Ellipsometry analysis was performed using two J. A. Woollam Co. systems, a V-VASE for the UV-VIS-NIR range (300 nm - 1700 nm) and a IR-VASE Mark-II for the MIR (1.7 μm – 20 μm). Ellipsometric parameters were taken at three angles (45º, 60º and 75º). The data from the two systems was combined and fitted to the modelled dielectric function over the whole spectral range (300 nm to 20 μm wavelength) using the WVASE software from J.A. Woollam Co.. For these experiments, the back of the samples was mechanically roughened to reduce reflections from the back surface. Two setups were employed for the electrical characterization of the films: the resistivity ρ was measured using a 4-point probe Jandel RM2 system in a linear configuration with a probe separation of 1 mm; resistivity and mobility, μ, were also characterized using a Nanometrics HL5500 Hall system in the Van der Pauw configuration.

RESULTS AND DISCUSSION

Ellipsometry

The ellipsometry data is fitted with a Tauc-Lorentz-Drude model (Figure 1a). The Tauc-Lorentz oscillator accounts for the band-to-band absorption and the properties in the UV-visible region of the spectrum, whilst the Drude oscillator accounts for the free carrier absorption in the infrared. Surface roughness and a thin layer of SiO_2 is included in the modelling.

For the ITO films grown at high temperatures a single homogeneous layer (plus roughness) is enough to produce a good fit between the experimental data and the model (Figure 1b and 1c). The calculated optical constants, presented in Figure 1 (f), are very similar in the three cases. Contrary to the films grown at high temperature, the films annealed required a graded layer to obtain a good fit. Figure 1 (h) shows the *n* and *k* data of the RT film and those annealed at 500 ºC and 600 ºC. The optical bandgap of the ITO varies considerably between samples. All the films grown at high temperature have the absorption edge at around 325 nm (3.81 eV), which is within the range of the reported data. The film grown at room temperature and those annealed show the absorption edge at nearly 400 nm (3.1 eV) and a significant variation between top and bottom of the film. This difference is generally attributed to a change in the carrier concentration [6].

The AZO films present a similar qualitative behaviour to the ITO films; a good fit is achieved using a homogeneous layer, but it requires an extra Lorentz-type oscillator in the MIR, in addition to the Drude component. Besides this unexpected component, which we associate to the existence of large in-plane inhomogeneities in the carrier densities, the optical-constant curves in Figure 1 (g) and (i) show that the absorption edge is almost independent of the deposition conditions or annealing process, being always in the 350-365 nm range (3.4-3.5 eV). They also demonstrate that the extinction coefficients are higher for the samples processed at higher temperatures, either grown or annealed, which is associated with an increase in the free carrier density and mobility compared to the samples processed at low temperature.

Hall and resistivity

The mobility and resistivity of the films were measured using the 4-point probe (4p) technique and Hall measurements, and derived from the Drude component of the models used to fit the ellipsometry data for each sample. These results are presented in Figure 2. For the annealed ITO samples, the calculated resistivities at the top and bottom of the film are included.

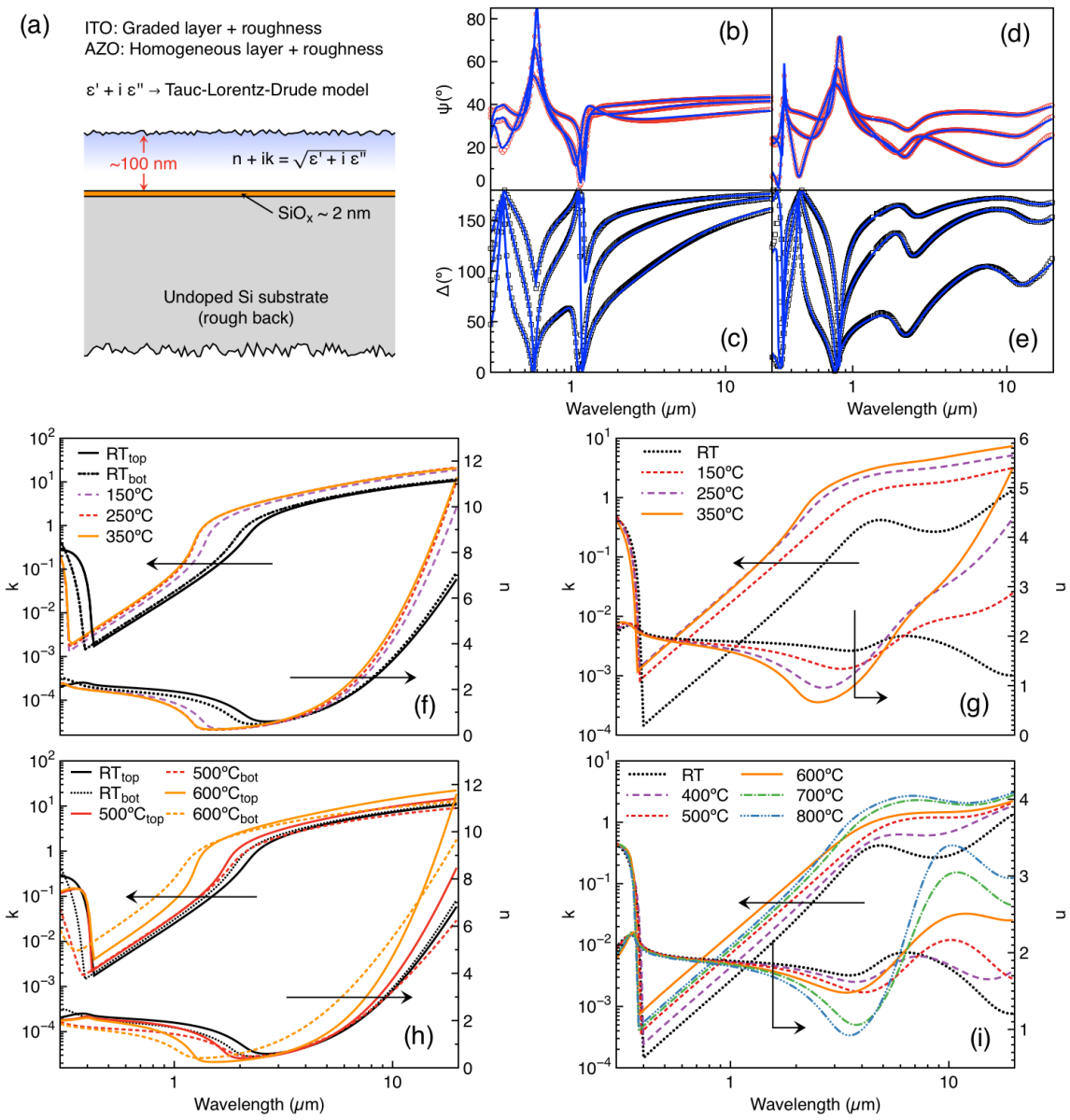

Figure 1. (a) Model of the sample structure used to fit the ellipsometry data. Experimental ellipsometric parameters (dots) and fit (blue line) of the ITO 250 ºC film - (b) and (c) – and the AZO 250 ºC film (d) and (e). The refractive index (*n*) and extinction coefficient (*k*) of ITO films grown at high temperature (f), selected, annealed ITO films (h), AZO films grown at high temperature (g) and annealed AZO films (i).

The resistivity of all ITO films is found to be between 0.1 and 1 mΩ-cm (Figure 2 (a)), with good general agreement between the three methods. Films grown at high temperature have the lowest resistivity from ~0.5 mΩ-cm for the film grown at 150 ºC to 0.2 mΩ-cm for that at 350 ºC. Dopant density deduced from Hall measurements (not shown) is around 1.3×10^{21} cm^{-3}. Films annealed at 800 ºC show a resistivity as low as 0.1 mΩ-cm near the top surface according to the ellipsometry results, but the average resistivity of the film as measured by 4p or Hall is around 0.3 mΩ-cm, as the bottom of the layers is much more resistive. In this case, the calculated dopant density is around 6×10^{20} cm^{-3}. Overall higher temperature processing yields to lower resistivity, with values of 0.1-0.2 mΩ-cm and in the range of the state of the art for ITO films [1].

For the AZO films grown at high temperature, the agreement between the resistivities obtained by the different techniques is in better agreement (Figure 2 (b)), producing values in the 10 to 1 mΩ-cm for the 150 ºC to 350 ºC samples, respectively, and Hall mobilities between 6 and 30 cm^2-V^{-1}-s^{-1}. These resistivities are at the higher end of the values often found in the literature [7]. Conversely, the resistivities obtained for annealed AZO films show significant discrepancies between the electrical and the optical measurements derived from the Drude model. The resistivities resulting from the latter are again lower than 10 mΩ-cm, decreasing with temperature down to 3 mΩ-cm for the 800 ºC film. Electrical measurements, however, demonstrate much higher values, up to 100 times higher in the case of the film annealed at 700 ºC. A non-obvious trend can be deduced from the dependence of the resistivity with the annealing temperature, which we associate to a strong electrical in-plane inhomogeneity of the films when the density of active dopants is low. Average dopant content as calculated with Hall for the AZO films is, indeed, more than one order of magnitude lower than for the ITO films, as low as 2×10^{19} cm^{-3} for the film annealed at 600 ºC.

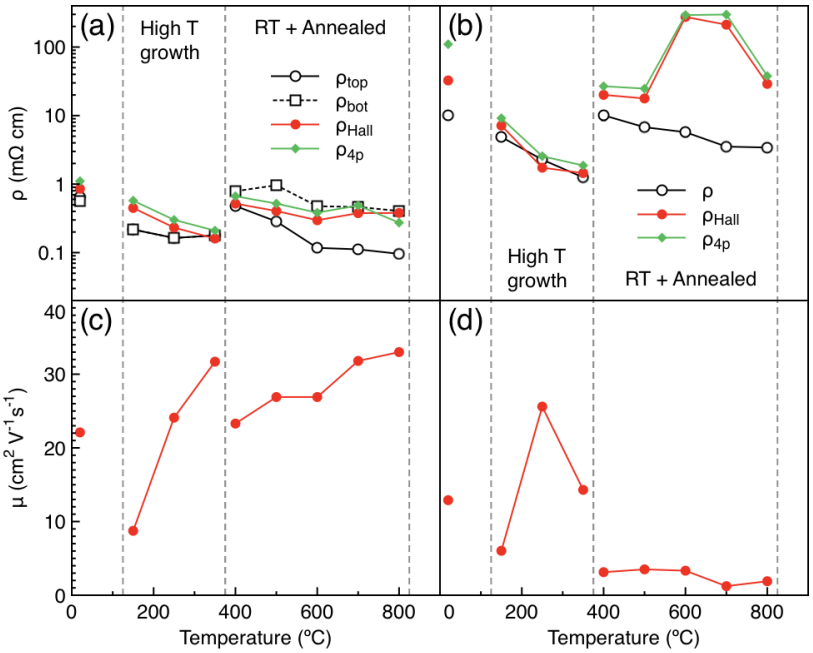

Figure 2. Resistivity, ρ, and mobility, μ, of the ITO (a) and (c) and AZO (b) and (d) films as measured with Hall, a 4 point probe and as derived from the ellipsometry fitting.

Assessment of performance of the low emissivity coatings

To assess the performance of the above films as low emissivity coatings we have used a transfer matrix algorithm to calculate how the radiation couples in and out of the solar cell – solar radiation in the visible and near-IR, and thermal radiation in the MIR. We use a stack made of the TCO film (variable thickness and material), highly doped silicon (450 μm, measured n and k) and a back surface of aluminum (200 nm, tabulated values). It is important that the suitability of the film is assessed together with the rest of the layers and not as a standalone material, given that the absorptivity (=emissivity) will depend on the optical properties of the structure as a whole. Compared with a real silicon solar cell, this three-layer planar structure has some simplifications, such as the lack of surface texture or thicker substrate. The main effect of this simplification is an overall reduction of the absorptivity and therefore the results presented here should be considered as a lower limit.

Figure 3 demonstrates the absorptivity results for TCO layers of different thicknesses calculated using the properties of the (a) ITO 250 ºC and (b) AZO 350 ºC films. Two distinct regions can be observed as a function of the wavelength associated with the regions where the TCOs are transparent and

absorptive. At short wavelengths, the films are transparent and light couples into the silicon substrate. Depending on the thickness of the layers, one or more interference fringes can be observed associated with regions of maximum and minimum reflection of the radiation. This is the usual observation from anti-reflecting coatings. At longer wavelengths, the films become both absorptive and highly reflective. In this range, increasing the film thickness reduces the absorptivity as the underlying silicon substrate is decoupled from the outside medium (air). Taking the optimal film thickness as the one giving the maximum light absorption above the silicon bandgap in order to maximize electrical output, we conclude that the optimal thicknesses for these films are 75 nm for ITO and 80 nm for AZO (Figure 3 (c)). The absorptivity in both cases is used to calculate the potential extracted power out of structures including these films as a function of the solar cell temperature. These are shown in Figure 3 (d) together with the results using the absorptivity of a commercial, diffused back surface field Si solar cell (the most common one in the market) [9] and the target emissivity that would be desirable for an optimum performance. An increase of 20% in the extracted power at 100 ºC compared to the silicon cell can be achieved in the case of AZO and over 50% for the ITO, demonstrating the potential of these films as low emissivity coatings to grow directly on silicon.

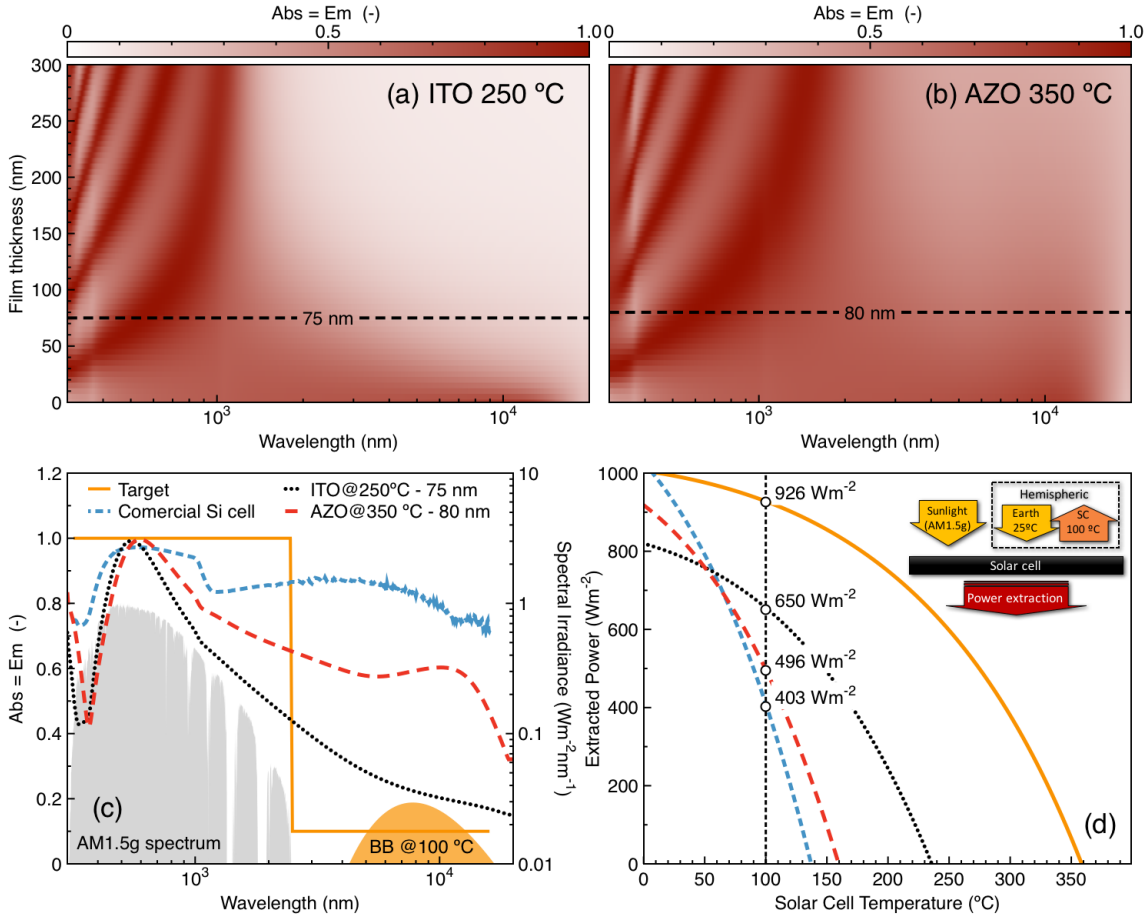

Figure 3. The calculated absorptivity using the ITO 250 ºC and AZO 350 ºC films using the three-layer model described in the text. (a) and (b) are absorptivity maps vs wavelength and film thickness. (c) Absorptivity at the optimum thickness, together with the absorptivity of a typical Si cell and the target emissivity. (d) Calculated extracted power for the target emissivity, the Si solar cell, and the optimal ITO and AZO films. The inset shows a schema of the power balanced model used.

CONCLUSIONS

In this work, we have presented a thorough analysis of the electrical and optical properties over a broad spectral range (300 nm to 20 μm) of ITO and AZO films fabricated and annealed at different temperatures intended for low thermal emissivity coating for silicon-based solar cells. Our results demonstrate that a single ITO layer, around 75 nm thick, deposited directly on the silicon substrate at 250 ºC allows for the best trade-off between sunlight transmittance into the solar cell, thermal emission suppression and electrical transport, resulting in an increase of the power extraction of over 50% compared to a silicon solar cell. AZO films, whilst showing superior transparency and sunlight coupling into the solar cell than ITO films, also demonstrate poorer electrical transport properties and thermal emission suppression. This result is a consequence of the specific deposition conditions used in this work, resulting in the AZO films being very close or even below the metal-insulator transition.

A final point to mention is the possibility of using multi-layer coatings to achieve even lower emissivity and keep good transparency in the visible. That is a common approach, and indeed the coating used by Lämmle et al., which reaches the best reported performance by using 6 layers including two AZO and one silver films [8]. By using a single layer, in this work we have favored the simplicity of fabrication and cost reduction of the ultimate final product. More importantly, it makes the low emissivity coating compatible with the role of the front electrode in solar cells – in particular of SHJ cells – something that is not possible in the previously reported multi-layered coatings.

ACKNOWLEDGMENTS

This work was funded by the Engineering and Physical Science Research council (EPSRC) grant EP/M025012/1. A. Mellor was supported by the European Commission through Marie Sklodowska Curie International Fellowship, Grant No. DLV-657359.

REFERENCES

1. K. Ellmer, *Nature Photon*, **6**, 1, (2012).
2. M. A. Green, *J Mater Sci: Mater Electron*, **18**, 15, (2007).
3. A. Khalil, Z. Ahmed, F. Touati, and M. Masmoudi. Proceedings of the 13th Int. Multi-Conference on Systems, Signals & Devices, 342 (2016).
4. A. Louwen, W. van Sark, R. Schropp, and A. Faaij, *Solar Energy Materials and Solar Cells*, **147**, 295, (2016).
5. D. Alonso-Álvarez, L. Ferre Llin, A. Mellor, D. J. Paul, and N. J. Ekins-Daukes, Submitted to *Solar Energy*, (2017) (unpublished).
6. S. Song, T. Yang, J. Liu, Y. Xin, Y. Li, and S. Han, *App. Surf. Sc.*, **257**, 7061, (2011).
7. A. K. Das, P. Misra, R. S. Ajimsha, A. Bose, S. C. Joshi, D. M. Phase, and L. M. Kukreja, *J. Appl. Phys*., **112**, 103706–7, (2012).
8. M. Lämmle, T. Kroyer, S. Fortuin, M. Wiese, and M. Hermann, *Solar Energy*, **130**, 161, (2016).
9. A. Riverola-Lacasta, A. Mellor, D. Alonso-Álvarez, L. Ferre Llin, I. Guarracino, A. Ramos Cabal, S. Thoms, C. N. Markides, D. J. Paul, N. J. Ekins-Daukes, and D. Chemisana, Submitted to *Progress in Photovoltaics* (2017) (unpublished)